USCAP

ARTICLE

Ubiquitin-specific protease 35 (USP35) mediates cisplatin-induced apoptosis by stabilizing BIRC3 in non-small cell lung cancer

Chunyan Liu[1], Zhaobo Chen[2], Xiaoyan Ding[1,3], Yun Qiao[4]✉ and Bing Li[1,5]✉

Ubiquitin-specific protease 35 (USP35) is a member of the ubiquitin-specific protease family (USP), which influences the progression of multiple cancers by deubiquitinating a variety of substrates. In recent years, the specific role of USP35 was begun to be understood. In this study, we investigated the role and underlying molecular mechanisms of USP35 in chemoresistance of non-small cell lung cancer (NSCLC) to cisplatin. Depletion of USP35 increased the sensitivity of NSCLC to cisplatin-induced apoptosis. We screened and identified a potential substrate of USP35, baculoviral IAP repeat containing 3 (BIRC3). Overexpression of USP35 in H460 cells increased the abundance of BIRC3, while USP35 knockdown in Anip973 cells decreased BIRC3 abundance. Notably, USP35 directly interacted with and stabilized BIRC3 through lys48-mediated polyubiquitination via its deubiquitinating enzyme activity. USP35 alleviated cisplatin-induced cell apoptosis by regulating BIRC3 levels in NSCLC cells. Moreover, a significant positive correlation between USP35 and BIRC3 protein expression levels was observed in human NSCLC tissues. Taken together, USP35 plays a vital role in resistance to cisplatin-induced cell death through the overexpression of BIRC3. USP35 might be a potentially novel therapeutic target in human NSCLC.

Laboratory Investigation (2022) 102:524–533; https://doi.org/10.1038/s41374-021-00725-z

INTRODUCTION

Lung cancer is the leading cause of cancer-related death worldwide, with an average 5-year survival rate of 15%[1,2]. Treatment of non-small cell lung cancer (NSCLC), which accounts for the majority of lung cancers, has achieved tremendous advances over the past two decades[3,4]. Surgery is recommended as a radical treatment for patients with NSCLC[5]. However, ~50% of patients are diagnosed with metastatic or locally advanced (Stage IIIB/IV) diseases[6]. Current treatment options for patients with metastatic or advanced lung cancer are limited, and the overall cure and survival rates of patients with NSCLC remain invariably low, particularly in patients with metastatic disease[7,8]. Therefore, further investigation of the molecular mechanisms underlying NSCLC progression is extremely effective to improve therapeutic outcomes and the overall survival of patients with NSCLC.

Ubiquitination regulates diverse cellular events through the modulation of protein metabolism and plays a pivotal role in various cellular processes[9–11]. Like other posttranslational modifications, ubiquitination is a reversible process mediated by deubiquitinating enzymes (DUBs)[12]. DUBs are divided into six classes based on their features: USPs (ubiquitin-specific proteases), UCHs (ubiquitin carboxy-terminal hydrolases), MJDs (Machado-Josephin domain-containing proteases), OTUs (ovarian tumor proteases), MINDYs (motif-interacting with ubiquitin-containing novel DUB family), and JAMMs (JAB1/MPN/MOV34 family)[13]. USPs are present in most forms of cancer, and ~60 USPs have been identified in humans that are closely related to the occurrence and development of a variety of cancers[14]. For example, USP3 plays a vital role in cell proliferation and spread by regulating cell cycle progression[15,16]. USP7 mediates the stabilization of the DNMT1 protein and plays a key role in the maintenance of DNA methylation[17]. USP28 stabilizes the oncogenic function of the LIN28a protein and regulates the c-Myc protein[18]. USP20 inhibits proliferation and delays the cell cycle of gastric cancer cells by regulating claspin[19].

Ubiquitin-specific protease 35 (USP35) is a member of the USP family, and its roles remain largely unknown. Existing reports have shown that USP35 regulates mitophagy by modulating MFN2 expression[20]. USP35 regulates cell mitosis by deubiquitinating and stabilizing Aurora B[21]. In addition, USP35 deubiquitinates STING and activates the STING-TBK1-IRF3 pathway in ovarian cancer[22]. As shown in our previous study, USP35 deubiquitinates ABIN-2 to inhibit the NF-κB signaling pathway[23]. In the present study, we aimed to detect the biological functions of USP35 in NSCLC.

In the present study, we screened and identified BIRC3 as a substrate of USP35. We confirmed that USP35 directly interacted with and deubiquitinated BIRC3, preventing its proteasome-dependent degradation. USP35 knockdown induced apoptosis and enhanced the sensitivity of lung cancer cells to cisplatin compared with controls, whereas BIRC3 or USP35 overexpression

[1]College of Basic Medicine, Qingdao University, Qingdao, China. [2]Department of Clinical Laboratory, Qilu Hospital, Shandong University, Qingdao, China. [3]Institute of Stem Cell and Regenerative Medicine, Qingdao University, Qingdao, China. [4]Department of Traditional Chinese Medicine, Qilu Hospital, Shandong University, Jinan, China. [5]Department of Hematology, The Affiliated Hospital of Qingdao University, Qingdao, China. ✉email: qiaoyun@qiluhospital.com; libing_516@qdu.edu.cn

Received: 18 July 2021 Revised: 10 December 2021 Accepted: 14 December 2021
Published online: 12 January 2022

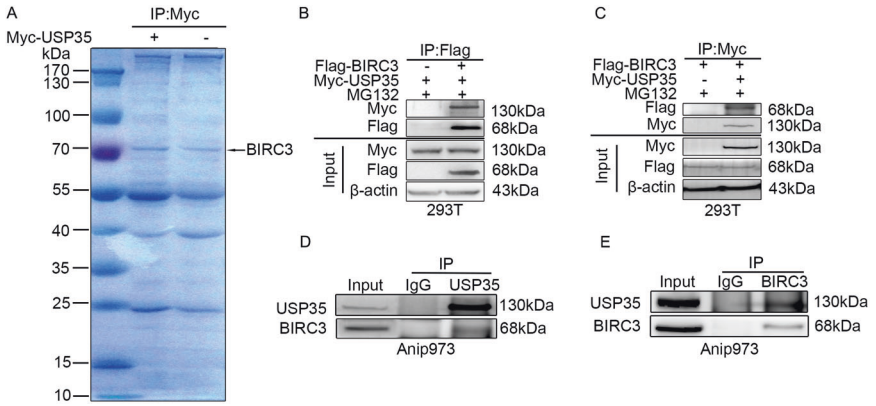

Fig. 1 USP35 interacts with BIRC3. A H460 cells were transiently transfected with the Myc vector or Myc-USP35 expression plasmid for 48 h. Cell lysates were purified, separated on gels and then stained with Coomassie blue R-250. A specific protein band was evaluated using mass spectrometric analysis. **B** HEK293T cells were transiently cotransfected with Myc-USP35 and Flag-BIRC3 or Flag-tagged control plasmids, and cell lysates were immunoprecipitated with an anti-Flag antibody followed by immunoblotting with an anti-Myc antibody. **C** HEK293T cells were transiently cotransfected with Flag-BIRC3 and Myc-USP35 or Myc-tagged control plasmids, and cell lysates were immunoprecipitated with an anti-Myc antibody followed by immunoblotting with an anti-Flag antibody. **D** Lysates of Anip973 cells were immunoprecipitated with an anti-USP35 or IgG antibody, followed by immunoblotting with an anti-BIRC3 antibody. **E** Lysates of Anip973 cells were immunoprecipitated with an anti-BIRC3 or IgG antibody, followed by immunoblotting with anti-USP35 antibody. All results are representative of three independent experiments.

rescued lung cancer cells from apoptosis induced by USP35 knockdown in the presence of cisplatin. USP35 and BIRC3 were positively correlated in human NSCLC tissues. Taken together, these data suggest a critical role for USP35 in chemoresistance by stabilizing BIRC3 in human lung cancer cells. Our findings indicate that USP35 may be an attractive molecular target for NSCLC therapy.

MATERIALS AND METHODS

Cell lines

Anip973 human NSCLC cells and HEK293T cells were purchased from GENE Biological Technology (Shanghai, China). H460 cells were kindly provided by Dr. Pengju Zhang. All the cells were cultured in RPMI-1640 medium supplemented with 10% fetal bovine serum (Invitrogen, Carlsbad, CA, USA) and 1% penicillin/streptomycin (Solarbio, Beijing, China). The growth conditions for all cells were 37 °C in an atmosphere of 95% air and 5% carbon dioxide.

Antibodies and reagents

The rabbit anti-USP35 antibody (ab86791, 1:3000) was purchased from Abcam (Cambridge, MA, USA). Rabbit anti-BIRC3 (3130 S, 1:1000) and rabbit anti-Myc (2272 S, 1:1000) antibodies were purchased from Cell Signaling Technologies (Danvers, MA, USA). The mouse anti-Flag antibody (F1804) was purchased from Sigma–Aldrich (St. Louis, MO, USA). Mouse anti-cleaved caspase-3 (19677, 1:2000) and rabbit anti-cleaved PARP1 (13371, 1:3000) antibodies were purchased from Proteintech Group, Inc. (Wuhan, China). Mouse anti-HA (sc-7392, 1:1000), mouse anti-β-actin (sc-1616, 1:1000) and secondary antibodies were purchased from Santa Cruz Biotechnology (Dallas, TX, USA). MG132 and cisplatin were purchased from Selleck PeproTech (Rocky Hill, NJ, USA). Protein A/G agarose was purchased from Santa Cruz (Dallas, TX, USA). Cycloheximide (CHX) was purchased from Calbiochem (Billerica, MA, USA). A protease inhibitor cocktail was purchased from Roche (Basel, Switzerland). Lipofectamine 2000 was obtained from Invitrogen (Grand Island, NY, USA). RIPA buffer was from Beyotime Biotechnology (Jiangsu, China).

Plasmids and transfection

USP35 and *BIRC3* full-length coding sequences were amplified from Anip973 cells using RT (reverse transcription)-PCR and cloned into 3 × Flag-, HA- or Myc-tagged fusion plasmids (Sigma). shRNAs and the small interfering RNA (siRNA) targeting human USP35 were designed and synthesized by GenePharma Company (Shanghai, China). shRNAs targeting USP35 were synthesized and subcloned into the pGPU6/GFP/Neo vector (GenePharma Company, Shanghai, China). All constructs were verified by DNA sequencing.

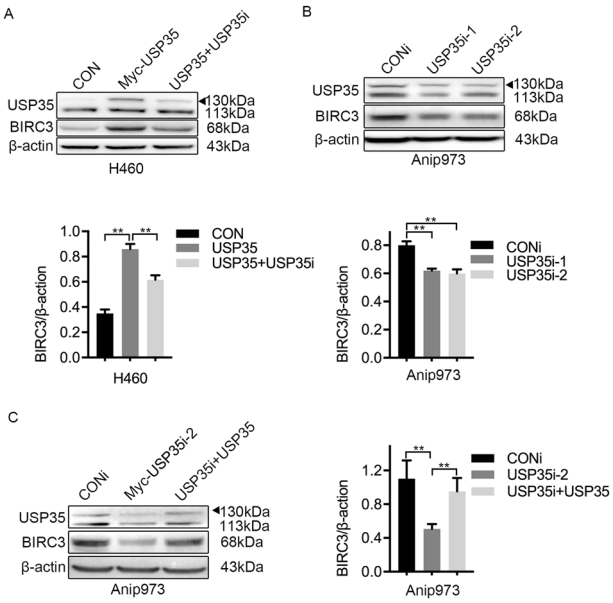

Fig. 2 USP35 upregulates the BIRC3 protein level. A The BIRC3 protein expression level in USP35-overexpressing or USP35 knock down H460 cells was detected using western blotting. **B** The BIRC3 protein expression level in USP35 knockdown Anip973 cells was detected using western blotting. **C** The USP35 expression plasmid or control plasmid was transfected into USP35 knockdown Anip973 cells. The BIRC3 protein expression level was detected using western blotting. All data are presented as means ± SD. *$P < 0.05$ and **$P < 0.01$ based on Student's t test. All results are representative of three independent experiments.

Transfections were performed using Lipofectamine™ 2000 according to the manufacturer's protocol. The siRNA or shRNA sequences for USP35 are as follows:

USP35-siRNA-1: 5′-GGGAAGATCTGATGATGTT-3′
USP35- siRNA-2: 5′-CCAAGAGGAAGGATGGTAC-3′
USP35-shRNA-3: 5′-GCTGAGTTGGGCTCTTC TAGA-3′
USP35-shRNA-4: 5′-GCGTCTGACTTCAGACATTG-3′.

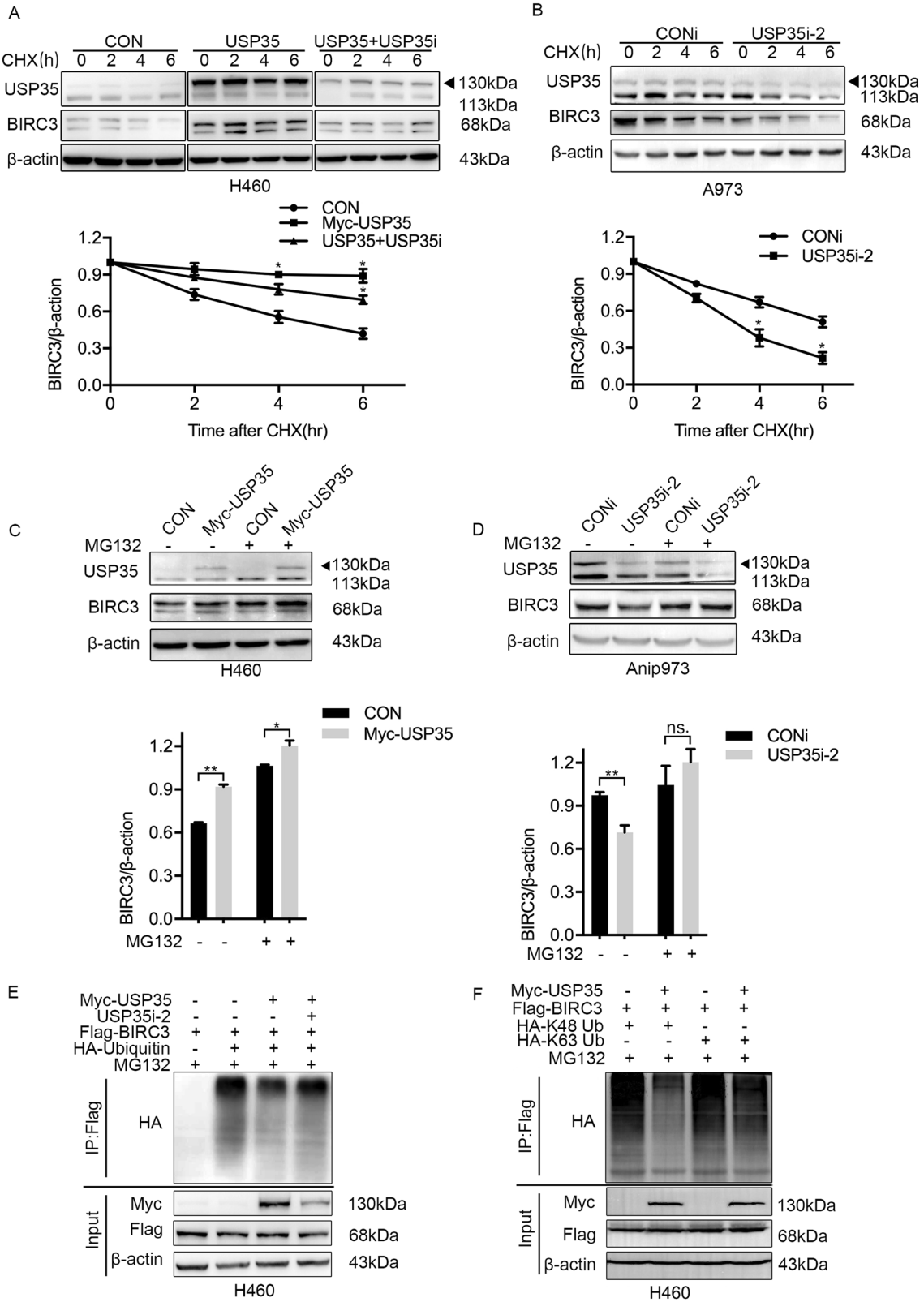

Western blot analysis

Total targeted cells were lysed using protein lysis buffer (Beyotime Biotechnology, Jiangsu, China) containing protease inhibitors (Roche, Indianapolis, IN, USA).

The proteins were separated on SDS–PAGE gels (10%) and then transferred to 0.45 μm polyvinylidene fluoride membranes (Millipore, Billerica, MA, USA). The membranes were immunoblotted with specific antibodies.

Coimmunoprecipitation

Briefly, the targeted cells were lysed using IP lysis buffer with protease inhibitors (Roche, Indianapolis, IN, USA). Approximately 2 mg of cell lysates

Fig. 3 USP35 deubiquitinates and stabilizes BIRC3. A and **B** H460 cells transfected with the USP35 overexpression plasmid, USP35 knockdown plasmid and control plasmid (**A**) and Anip973 cells transfected with siRNA USP35i-2 and the control siRNA (**B**) were treated with 50 μg/ml cycloheximide (CHX) for 0, 2, 4 and 6 h. The BIRC3 protein expression level was detected using western blotting. The quantitative analysis of the CHX-chase assay results is shown in the figure. **C** and **D** H460 cells transfected with the USP35 overexpression plasmid and control plasmid (**C**) and Anip973 cells transfected with siRNA USP35i-2 and the control siRNA (**D**) were treated with or without 10 μM MG132 for 6 h. The BIRC3 protein expression level was detected using western blotting. The quantitative analysis is shown in the figure. **E** HA-tagged ubiquitin and Flag-BIRC3 were cotransfected into H460 cells in the presence of Myc-USP35 or USP35 knockdown plasmid. Cell lysates were immunoprecipitated with an anti-Flag antibody, followed by immunoblotting with an anti-HA antibody. **F** K48- or K63-linked polyubiquitin chains and Flag-BIRC3 overexpression plasmid were cotransfected into H460 cells in the presence of wild-type Myc-USP35 or control vector. Cell lysates were immunoprecipitated with an anti-Flag antibody, followed by immunoblotting with an anti-HA antibody. All data are presented as means ± SD. $^{*}P < 0.05$ and $^{**}P < 0.01$ based on Student's *t* test. All results are representative of three independent experiments.

were incubated with the indicated target-specific antibodies overnight at 4 °C on a vertical roller. Next, the lysates were incubated with 30 μl of Protein A/G agarose beads for 4 h, and the immunocomplexes were washed five times with cold lysis buffer and boiled in 2 × SDS sample buffer. All samples were detected using western blot analysis with the corresponding primary antibodies, and 5% of the samples were used to identify the immunoprecipitation efficiency.

Flow cytometry analysis

The Annexin V-FITC Apoptosis Detection Kit (Bestbio, Shanghai, China) was used to detect the apoptosis of Anip973 cells after transfection with the indicated plasmids for 48 h in the presence or absence of cisplatin treatment. The targeted cells were digested using 0.25% trypsin without EDTA, washed two times with cold PBS, and then resuspended in precooled Annexin V binding solution at 4 °C. The density of cells in each sample was ~1×10^6 cells/ml. The cells were incubated in the dark with Annexin V-FITC and propidium iodide for 10 min at 2–8 °C. Cell apoptosis was measured using a BD Biosciences FACSCanto II Analyzer.

Terminal dUTP nick-end labeling (TUNEL) assay

The TUNEL Detection Kit (KeyGEN Biotech, Nanjing, China) was used to detect DNA integrity after transfection with the indicated plasmids and treatment with or without cisplatin. The slices were fixed with 4% paraformaldehyde and then incubated in the dark with 50 μl of labeling reaction mixture (1 μl of biotin-11-dUTP, 4 μl of TdT enzyme and 45 μl of equilibration buffer) for 60 min and with 50 μl of labeling mixture (5 μl of streptavidin-TRITC and 45 μl of labeling buffer) for 30 min at 37 °C in a humid chamber. The cells in slices were counterstained with DAPI (Beyotime Biotechnology, Jiangsu, China) for 10 min and visualized using fluorescence microscopy.

CHX chase assay

A CHX chase assay was performed to detect protein stability. Cells were transfected with the indicated plasmids for 48 h, treated with CHX (50 μg/ml) and harvested at the indicated time points. Treated cells were collected and lysed using protein lysis buffer, and the lysates were detected using western blotting with anti-BIRC3 or anti-β-actin antibodies.

Immunohistochemical analysis

Forty pairs of NSCLC tissue specimens and adjacent noncancerous tissue specimens were obtained from patients undergoing surgical excision of tumors in the Affiliated Hospital of Qingdao University (Qingdao, China). Informed consent was obtained from all patients for inclusion in the study. Briefly, the paraffin-embedded sections were dewaxed and rehydrated, and then antigen retrieval was performed with citrate buffer (ZSGB-BIO, Beijing, China) in a microwave. Primary antibodies were added to sections and incubated at 4 °C overnight. The next day, sections were incubated with the enhancer solution and appropriate secondary antibody for 20 min and then stained with 3,3′-diaminobenzidine and hematoxylin. The expression patterns were evaluated based on the intensity and proportion of staining in tumor cells. The scores for immunohistochemical staining were assessed by two pathologists.

Statistical analysis

GraphPad Prism 8 software (La Jolla, CA, USA) was used for statistical analyses. All data are presented as the means ± SD of at least three independent experiments. Different groups were compared a two-tailed unpaired Student's *t* test. Spearman's correlation analysis was performed to assess the correlation between USP35 and BIRC3 expression in NSCLC tissues using a multivariate Cox regression analysis. $P < 0.05$ was considered statistically significant.

RESULTS

USP35 interacts with BIRC3

We performed an immunoprecipitation assay and mass spectrometry analysis to search for the proteins and novel substrates that associated with USP35 in H460 cells transfected with the Myc-tagged USP35 expression plasmid or empty vector plasmid. The mass spectrometry analysis indicated that BIRC3 was copurified with Myc-tagged USP35 (Fig. 1A).

We validated this result by performing a coimmunoprecipitation (Co-IP) analysis to test the interaction between USP35 and BIRC3. HEK293T cells were transiently cotransfected with Myc-USP35 and Flag-BIRC3 or Flag-tagged control plasmids, and lysates were immunoprecipitated with an anti-Flag antibody followed by immunoblotting with an anti-Myc antibody. On the other hand, HEK293T cells were transiently cotransfected with Flag-BIRC3 and Myc-USP35 or Myc-tagged control plasmids, and lysates were immunoprecipitated with an anti-Myc antibody followed by immunoblotting with an anti-Flag antibody. Myc-tagged USP35 interacted with Flag-tagged BIRC3 (Fig. 1B, C). Furthermore, Anip973 cell lysates were purified with an anti-USP35 or anti-BIRC3 antibody followed by immunoblotting with an anti-BIRC3 or anti-USP35 antibody to examine the interaction between endogenous USP35 and BIRC3. Consistently, endogenous USP35 was associated with endogenous BIRC3 in Anip973 cells (Fig. 1D, E). These results indicated that USP35 directly interacted with BIRC3.

USP35 regulates the levels of the BIRC3 protein

Myc-USP35 expression plasmid and empty vector plasmid were transfected into H460 cells to further validate the regulatory effect of USP35 on BIRC3 in NSCLC cells. Ectopic expression of USP35 significantly increased the expression of BIRC3, while USP35 knockdown in H460-USP35 cells decreased the expression of BIRC3 (Fig. 2A). Next, siRNAs targeting USP35 (USP35i-1 and USP35i-2) and a control siRNA were transfected into Anip973 cells. USP35 knockdown strongly suppressed BIRC3 expression compared to the control siRNA treatment (Fig. 2B). Accordingly, overexpression of USP35 in Anip973-siUSP35 cells restored BIRC3 expression (Fig. 2C). These data proved that USP35 upregulated BIRC3 protein levels.

USP35 regulates BIRC3 stability in a proteasome-dependent manner

BIRC3 protein turnover in H460 cells and Anip973 cells transfected with the indicated plasmids was measured by performing a CHX chase assay to investigate the regulatory mechanism by which USP35 upregulates BIRC3 protein expression. The half-life of BIRC3 was significantly extended when USP35 expression was increased, while USP35 knockdown in H460-USP35 cells increased degradation of BIRC3 (Fig. 3A), more rapid degradation of the BIRC3 protein was also observed after the depletion of USP35 in Anip973

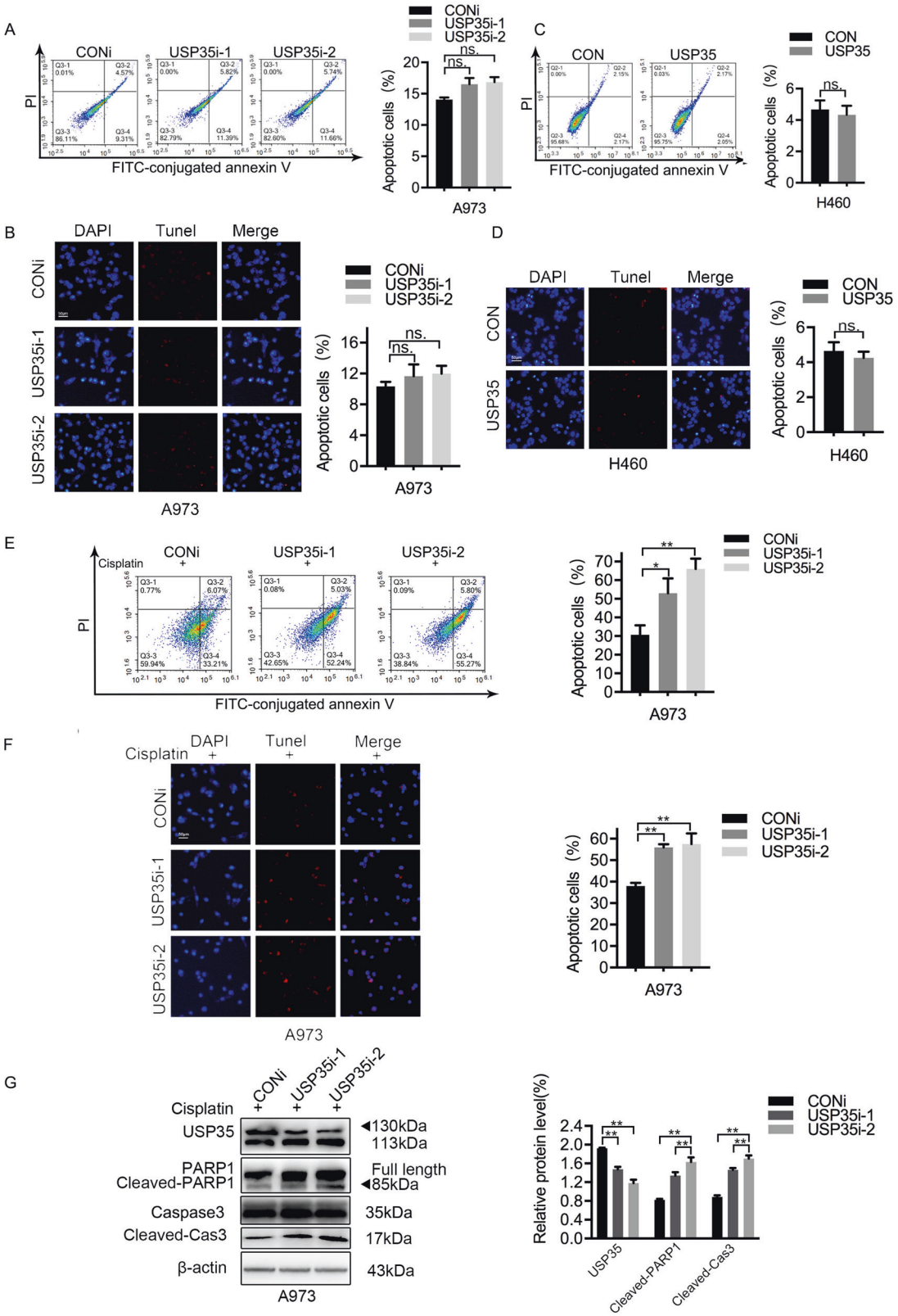

cells than in the control group (Fig. 3B). Based on these results, USP35 upregulates BIRC3 expression by preventing its degradation. Then, we explored whether USP35 prevented the degradation of BIRC3 through a proteasome-dependent pathway. H460 cells with USP35 overexpression or Anip973 cells with USP35 knockdown were treated with or without the proteasome inhibitor MG132. Western blot analysis showed significantly increased levels of the BIRC3 protein in both CON- and USP35-transfected H460 cells in the presence of MG132 (Fig. 3C). Meanwhile, the proteasome inhibitor MG132 blocked the USP35 silencing-

Fig. 4 USP35 regulates cisplatin-induced cell apoptosis. A Anip973 cells were transfected with USP35-specific siRNAs (USP35i-1 and USP35i-2) or the control siRNA (CONi) for 48 h. The cells were stained with Annexin V-FITC and propidium iodide (PI) and analyzed using flow cytometry. The quantitative analysis is shown in the figure. **B** Anip973 cells were transfected with USP35-specific siRNAs (USP35i-1 and USP35i-2) or the control siRNA (CONi) for 48 h. Cells were detected using TUNEL staining. The quantitative analysis is shown in the figure. **C** H460 cells were transfected with USP35-expression plasmid or the control plasmid for 48 h. The cells were stained with Annexin V-FITC and propidium iodide (PI) and analyzed using flow cytometry. The quantitative analysis is shown in the figure. **D** H460 cells were transfected with USP35-expression plasmid or the control plasmid for 48 h. Cells were detected using TUNEL staining. The quantitative analysis is shown in the figure. **E** Anip973 cells transfected with USP35-specific siRNAs (USP35i-1 and USP35i-2) or the control siRNA (CONi) were treated with cisplatin for 24 h. Cells were stained with Annexin V-FITC and propidium iodide (PI) and analyzed using flow cytometry. The quantitative analysis is shown in the figure. **F** Anip973 cells transfected with USP35-specific siRNAs (USP35i-1 and USP35i-2) or the control siRNA (CONi) were treated with cisplatin for 24 h. Cells were detected using TUNEL staining. The quantitative analysis is shown in the figure. **G** Anip973 cells transfected with USP35-specific siRNAs (USP35i-1 and USP35i-2) or the control siRNA (CONi) were treated with cisplatin for 24 h. The proteins listed above were detected using western blotting. The quantitative analysis is shown in the figure. All data are presented as means ± SD. $^{*}P < 0.05$ and $^{**}P < 0.01$ based on Student's *t* test. All results are representative of three independent experiments.

induced decrease in BIRC3 levels (Fig. 3D). These results illustrated that USP35 protected the BIRC3 protein from proteasomal degradation.

Since USPs usually stabilize their substrates by deubiquitination, we investigated whether USP35 deubiquitinated BIRC3. HA-tagged ubiquitin and Flag-BIRC3 were cotransfected into H460 cells in the presence of Myc-USP35 or USP35 knockdown plasmid. Immunoprecipitation assays showed that USP35 significantly decreased the level of BIRC3 ubiquitination, whereas USP35 knockdown plasmid rescued BIRC3 ubiquitination induced by USP35 overexpression (Fig. 3E). We performed a deubiquitination assay in H460 cells cotransfected with HA-K48- or HA-K63-ubiquitin plasmids, Flag-BIRC3 expression plasmids and Myc-USP35 plasmids or control vector to identify the linkage types of ubiquitin chains on BIRC3. USP35 significantly decreased the level of BIRC3 ubiquitination in cells transfected with HA-K48 ubiquitin but did not decrease the level of BIRC3 ubiquitination in cells transfected with HA-K63 ubiquitin, indicating that USP35 cleaves the K48-linked ubiquitin from BIRC3 (Fig. 3F).

Taken together, these results showed that USP35 promoted the deubiquitination of BIRC3 and stabilized BIRC3 in a proteosome-dependent manner.

USP35 knockdown increases chemosensitivity in NSCLC cells

As BIRC3 is identified as a candidate target of USP35 and has been reported to be involved in chemotherapy resistance and to be associated with cisplatin-induced apoptosis, we speculated that USP35 may also participate in regulating cell apoptosis and chemotherapy sensitivity in NSCLC cells. We performed a flow cytometry analysis and TUNEL assays to detect the effects of USP35 on cell apoptosis and confirm the roles of USP35 in NSCLC. First, Anip973 cells were transfected with USP35i-1 and USP35i-2 and stained with Annexin V/PI for flow cytometry analysis. Results of the flow cytometry analysis showed that USP35 knockdown led to a slight increase in apoptosis (Fig. 4A). Consistent with the flow cytometry data, the TUNEL assay also revealed a slight increase in apoptosis in USP35 knockdown Anip973 cells (Fig. 4B), indicating that USP35 had no significant effects on cell apoptosis in the resting state. Results of the flow cytometry analysis and the TUNEL assay detected in H460 cells also revealed that USP35 had no significant effects on cell apoptosis in the resting state. (Fig. 4C, D) Next, we investigated the effects of USP35 on the cisplatin-induced apoptosis of NSCLC cells. Flow cytometry and TUNEL assays were employed to detect the apoptosis of Anip973 cells transfected with USP35i-1 and USP35i-2 and cultured in the presence of cisplatin. The flow cytometry analysis showed that USP35 knockdown significantly increased apoptosis in the presence of cisplatin (Fig. 4E), and we also observed a reduction in apoptosis after co-transfection with the USP35 overexpression plasmid (Fig. 5A). Consistent with the flow cytometry data, the TUNEL assay also revealed a remarkable increase in apoptosis in USP35 knockdown Anip973 cells (Fig. 4F) and a reduction in apoptosis after co-transfection with the USP35 overexpression plasmid (Fig. 5B). These results were further confirmed by detecting the levels of apoptosis-related markers, cleaved PARP and caspase-3, using western blotting (Figs. 4G, 5C). Taken together, these results show that USP35 knockdown substantially improved cisplatin sensitivity in Anip973 cells.

USP35 affects cisplatin-induced cell apoptosis through BIRC3

We further confirmed whether USP35 regulated the chemoresistance of NSCLC cells to cisplatin through the BIRC3 protein by transfecting Anip973 cells with USP35i-2 alone or in combination with BIRC3 expression plasmids and culturing them in the presence of cisplatin. Results of the flow cytometry and TUNEL assays showed that USP35-silenced cells exhibited sensitivity to cisplatin treatment and significantly increased apoptosis after treatment with cisplatin compared with the control cells, whereas the BIRC3 overexpression plasmid rescued apoptosis induced by USP35 knockdown (Fig. 5A, B). We detected the levels of the apoptosis-related markers PARP and caspase-3 in cells treated as mentioned above using western blot analysis. Western blot results showed that cleavage of PARP and caspase-3 was significantly increased in Anip973 cells with USP35 knockdown after cisplatin treatment compared with that in control cells, whereas ectopic expression of BIRC3 abrogated the increased cleavage of PARP and caspase-3 proteins induced by USP35 knockdown (Fig. 5C). Based on these data, USP35 influenced the outcome of chemotherapy in NSCLC cells treated with cisplatin by regulating BIRC3 expression.

USP35 expression is positively correlated with BIRC3 expression in human NSCLC tissues

Finally, we analyzed the expression of USP35 and BIRC3 in NSCLC tissues and adjacent noncancerous tissues to determine their clinical association. Immunohistochemistry (IHC) was performed using antibodies against USP35 and BIRC3 in 40 pairs of NSCLC tissue specimens and adjacent noncancerous tissue specimens. Both USP35 and BIRC3 showed increased expression in NSCLC tissues compared with adjacent noncancerous tissues (Fig. 6A). In the 40 NSCLC tissue samples tested, quantification of the immunostaining and statistical analysis showed a significant positive correlation between USP35 and BIRC3 (Fig. 6B–D).

DISCUSSION

Recently, an increasing number of studies have shown that USPs are present in multiple tumor types and are involved in regulating the progression and drug resistance of multiple tumor types. For example, downregulation of USP1 effectively sensitizes NSCLC and osteosarcoma cells to cisplatin, which may be a potential drug target in tumors with cisplatin resistance[24]. USP7 silencing reduces CCDC6 levels to increase the sensitivity of bladder cancer cells to olaparib[25]. Loss of USP9X leads to tamoxifen resistance in breast

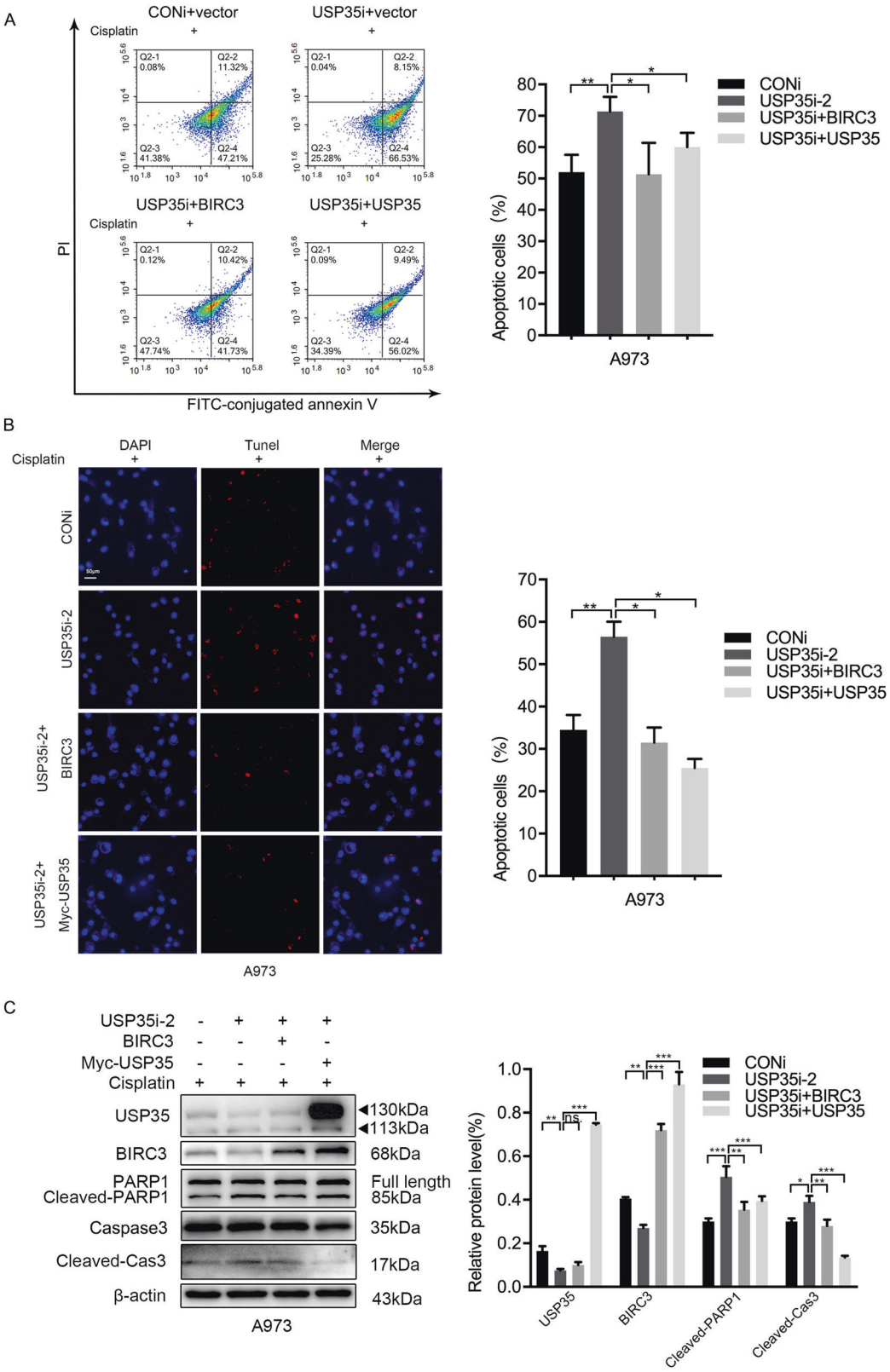

cancer cells and promotes cell proliferation[26]. Treatment with USP14 inhibitors induces apoptosis in multiple myeloma cells and overcomes resistance to bortezomib[27]. These findings suggest crucial roles for DUBs in the chemoresistance of multiple cancer types.

USP35 is a new member of the USP family. Existing research has revealed that USP35 regulated cancer cell progression, including proliferation, mitosis and malignant progression. However, to our knowledge, no report on the effects of USP35 on the sensitivity of NSCLC cells to chemotherapeutics is currently available.

Fig. 5 USP35 affects cisplatin-induced cell apoptosis through BIRC3 regulation. A Anip973 cells were transfected with USP35i-2 alone or in combination with the BIRC3 overexpression plasmid or in combination with the USP35 overexpression plasmid for 24 h, and then the cells were treated with cisplatin for 24 h. The cells were stained with Annexin V-FITC and propidium iodide (PI) and analyzed using flow cytometry. The quantitative analysis is shown in the figure. **B** Anip973 cells were transfected with USP35i-2 alone or in combination with the BIRC3 overexpression plasmid or the USP35 overexpression plasmid for 24 h, and then the cells were treated with cisplatin for 24 h. Cells were detected using TUNEL staining. The quantitative analysis is shown in the figure. **C** Anip973 cells were transfected with USP35i-2 alone or in combination with the BIRC3 overexpression plasmid or the USP35 overexpression plasmid for 24 h and then treated with cisplatin for 24 h. The proteins mentioned above were detected using western blotting. The quantitative analysis is shown in the figure. All data are presented as means ± SD. $^{*}P < 0.05$, $^{**}P < 0.01$, and $^{***}P < 0.001$ based on Student's *t* test. All results are representative of three independent experiments.

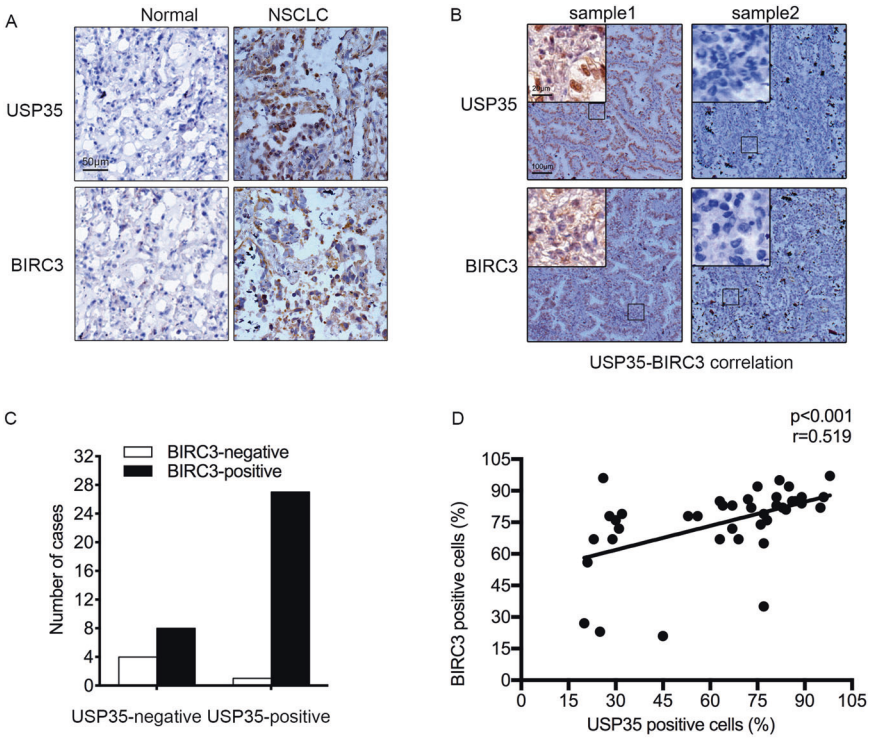

Fig. 6 BIRC3 expression is positively correlated with USP35 expression in NSCLC tissues. A USP35 and BIRC3 protein expression levels in adjacent noncancerous tissue specimens and NSCLC tissue specimens were analyzed using immunohistochemistry (IHC), and representative images are shown. **B** USP35 and BIRC3 protein expression levels in NSCLC tissues were analyzed using IHC, and representative images are shown. **C** The graphs show the relative BIRC3 level in USP35-negative and USP35-positive NSCLC tissues. **D** The scatter plot presents the correlation between USP35 and BIRC3 expression in NSCLC tissues ($n = 40$).

As DUBs usually exert their biological functions by modulating different target proteins, we screened the potential substrates of USP35 through immunoprecipitation and mass spectrometry analysis. BIRC3 was identified among the copurified proteins and validated with a subsequent Co-IP assay. Western blot results showed that BIRC3 expression was regulated by USP35 in different NSCLC cells with USP35 overexpression or knockdown. We then analyzed the molecular mechanism by which USP35 regulates BIRC3 expression. USP35 physically interacts with BIRC3 and regulates the stability of BIRC3. BIRC3 is more stable in USP35-overexpressing cells, while BIRC3 is degraded more quickly in USP35 knockdown cells. USP35 overexpression decreases the level of BIRC3 ubiquitination. These data confirm that BIRC3 is a real target of USP35 that is deubiquitinated and stabilized at the protein level by USP35.

BIRC3 is a member of the inhibitor of apoptosis (IAP) protein family, which may inhibit apoptosis by targeting caspases to promote cellular survival in cancers[28]. For example, downregulation of BIRC3 significantly promotes apoptosis by directly inhibiting caspase-3 in Hodgkin lymphoma cells[29]. BIRC3 knockdown significantly reduces the proliferation and invasion of BEL7402 and HepG2 cells and the activity of the NF-κB pathway[30]. BIRC3 is critical to maintain a normal innate immune inflammatory response[31]. In addition, BIRC3 overexpression is associated with chemoresistance and the poor prognosis of patients with multiple cancer types. For example, the downregulation of BIRC3 significantly increases apoptosis by sensitizing colorectal cancer and oral squamous cell carcinoma cells to 5-fluorouracil[32,33]. BIRC3 is an important factor mediating bortezomib resistance in multiple myeloma cells and human melanoma[34,35]. Inhibition of BIRC3 significantly enhances cisplatin sensitivity in ovarian cancer and lung cancer cells[36–38]. Thus, an understanding of the regulatory mechanism of BIRC3 is important for cancer control.

Cisplatin, the first-line antitumor drug, has been used to treat multiple human cancers, including bladder, lung, endometrium, ovarian, colon, prostate and brain cancers, by inducing tumor cell apoptosis[39–41]. However, the therapeutic effect of cisplatin is limited by drug resistance during the treatment process. For example, excision repair cross-complementing 1 (ERCC1), a nucleotide excision repair protein, is linked to cisplatin resistance[42–44]. Hypoxia-induced overexpression of HIF-1α and HIF-2α has been reported to negatively affect the therapeutic efficacy of cisplatin in NSCLC[45–48]. Moreover, nuclear factor erythroid

2-related factor 2 (Nrf2) plays a pivotal role in cisplatin drug resistance in NSCLC cells[49,50]. Glutathione, an important cellular antioxidant, alters the sensitivity of NSCLC cells to cisplatin[51]. In view of the key role of BIRC3 in regulating cisplatin-induced apoptosis and the interaction between USP35 and BIRC3, we detected that USP35 knockdown enhanced the sensitivity of Anip973 cells to cisplatin-induced apoptosis using flow cytometry and TUNEL assays. In contrast, BIRC3 overexpression in USP35 knockdown Anip973 cells reversed this phenomenon in the presence of cisplatin. Western blot results showed that in the presence of cisplatin, USP35 silencing increased the levels of cleaved caspase-3 and cleaved PARP1, while BIRC3 overexpression reduced the levels of the abovementioned proteins in USP35 knockdown Anip973 cells. These results confirmed that USP35 played an important role in cisplatin-induced apoptosis in NSCLC cells and provided evidence that downregulation of USP35 is a novel mechanism to sensitize lung cancer cells to cisplatin treatment. In addition, our current study found that USP35 knockdown increased sensitivity to cisplatin by regulating the expression of the antiapoptotic protein BIRC3 in lung cancer. Combination treatment with drugs targeting USP35 and chemotherapy drugs such as cisplatin may synergistically enhance the antitumor effects. Future studies should include an investigation of USP35-mediated regulation of BIRC3 in mouse tumorigenesis models and drug-resistant cell line models to further elucidate the molecular mechanisms of USP35 in chemoresistance.

In summary, our study revealed that USP35 interacts with and deubiquitinates BIRC3. In addition, the depletion of USP35 enhances the sensitivity of NSCLC cells to cisplatin by decreasing the stability of BIRC3. Given the chemosensitizing effect of USP35 knockdown on NSCLC in this study, USP35 may represent a potential molecular target to be combined with other chemotherapeutic strategies for treating patients with NSCLC.

DATA AVAILABILITY

The data used to support the findings of this study are included within the paper.

REFERENCES

1. Molina, J. R., Yang, P., Cassivi, S. D., Schild, S. E. & Adjei, A. A. Non-small celllung cancer: epidemiology, risk factors, treatment, and survivorship. *Mayo Clin. Proc.* **83**, 584–594 (2008).
2. Hong, Q. Y. et al. Prevention and management of lung cancer in China. *Cancer* **121**, 3080–3088 (2015).
3. Herbst, R. S., Morgensztern, D. & Boshoff, C. The biology and management of non small cell lung cancer. *Nature* **553**, 446–454 (2018).
4. Giustini, N. P., Jeong, A. R., Buturla, J. & Bazhenova, L. Advances in Treatment of Locally Advanced or Metastatic Non-Small Cell Lung Cancer: targeted therapy. *Clin. Chest Med.* **41**, 223–235 (2020).
5. Samson, P. et al. Interpreting survival data from clinical trials of surgery versus stereotactic body radiation therapy in operable Stage I non-small cell lung cancer patients. *Lung Cancer* **103**, 6–10 (2017).
6. Beckett, P., Tata, L. J. & Hubbard, R. B. Risk factors and survival outcome for non elective referral in non-small cell lung cancer patients–analysis based on the National Lung Cancer Audit. *Lung Cancer* **83**, 396–400 (2014).
7. Miller, K. D. et al. Cancer treatment and survivorship statistics, 2019. *CA Cancer J. Clin.* **69**, 363–385 (2019).
8. Xiao, Y. et al. FBXW7 deletion contributes to lung tumor development and confers resistance to gefitinib therapy. *Mol. Oncol.* **12**, 883–895 (2018).
9. Swatek, K. N. et al. Insights into ubiquitin chain architecture using Ub-clipping. *Nature* **572**, 533–537 (2019).
10. Swatek, K. N. & Komander, D. Ubiquitin modifications. *Cell Res.* **26**, 399–422 (2016).
11. Clague, M. J. & Urbé, S. Integration of cellular ubiquitin and membrane traffic systems: focus on deubiquitylases. *Febs J.* **284**, 1753–1766 (2017).
12. Hershko, A. The ubiquitin system for protein degradation and some of its roles in the control of the cell division cycle. *Cell Death Differ* **12**, 1191–1197 (2005).
13. Harrigan, J. A., Jacq, X., Martin, N. M. & Jackson, S. P. Deubiquitylating enzymes and drug discovery: emerging opportunities. *Nat. Rev. Drug Discov.* **17**, 57–78 (2018).
14. Tanguturi, P., Kim, K. S. & Ramakrishna, S. The role of deubiquitinating enzymes in cancer drug resistance. *Cancer Chemother. Pharmacol.* **85**, 627–639 (2020).
15. Fang, C. L. et al. Ubiquitin-specific protease 3 overexpression promotes gastric carcinogenesis and is predictive of poor patient prognosis. *Cancer Sci.* **109**, 3438–3449 (2018).
16. Wu, Y. Y. et al. USP3 promotes breast cancer cell proliferation by deubiquitinating KLF5. *J. Biol. Chem.* **294**, 17837–17847 (2019).
17. Cheng, J. D. et al. Molecular mechanism for USP7-mediated DNMT1 stabilization by acetylation. *Nat. Commun.* **6**, 7023 (2015).
18. Haq, S. et al. The stability and oncogenic function of LIN28A are regulated by USP28. *Biochim. Biophys. Acta Mol. Basis Dis.* **1865**, 599–610 (2019).
19. Wang, C. et al. Deubiquitinating enzyme USP20 is a positive regulator of Claspin and suppresses the malignant characteristics of gastric cancer cells. *Int. J. Oncol.* **50**, 1136–1146 (2017).
20. Wang, Y. Q. et al. Deubiquitinating enzymes regulate PARK2-mediated mitophagy. *Autophagy* **11**, 595–606 (2015).
21. Park, J. Y., Kwon, M. S., Kim, E. E., Lee, H. & Song, E. J. USP35 regulates mitotic progression by modulating the stability of Aurora B. *Nat. Commun.* **9**, 688 (2018).
22. Zhang, J. W. et al. Deubiquitinase USP35 restrains STING-mediated interferon signaling in ovarian cancer. *Cell Death Differ.* **28**, 139–155 (2021).
23. Liu, C. Y. et al. USP35 activated by miR let-7a inhibits cell proliferation and NF-Kb activation through stabilization of ABIN-2. *Oncotarget* **6**, 27891–27906 (2015).
24. Liang, Q. et al. A selective USP1-UAF1 inhibitor links deubiquitination to DNA damage responses. *Nat. Chem. Biol.* **10**, 298–304 (2014).
25. Morra, F. et al. CCDC6 and USP7 expression levels suggest novel treatment options in high-grade urothelial bladder cancer. *J. Exp. Clin. Cancer Res.* **38**, 90 (2019).
26. Oosterkamp, H. M. et al. USP9X downregulation renders breast cancer cells resistant to tamoxifen. *Cancer Res.* **74**, 3810–3820 (2014).
27. Tian, Z. et al. A novel small molecule inhibitor of deubiquitylating enzyme USP14 and UCHL5 induces apoptosis in multiple myeloma and overcomes bortezomib resistance. *Blood* **123**, 706–716 (2014).
28. Fulda, S. & Vucic, D. Targeting IAP proteins for therapeutic intervention in cancer. *Nat. Rev. Drug Discov.* **11**, 109–124 (2012).
29. Dürkop, H., Hirsch, B., Hahn, C. & Stein, H. cIAP2 is highly expressed in Hodgkin Reed-Sternberg cells and inhibits apoptosis by interfering with constitutively active caspase-3. *J. Mol. Med. (Berl)* **84**, 132–141 (2006).
30. Jiang, X. J. et al. cIAP2 via NF-κB signalling affects cell proliferation and invasion in hepatocellular carcinoma. *Life Sci.* **266**, 118867 (2021).
31. Zhang, J. et al. Ubiquitin Ligases cIAP1 and cIAP2 Limit Cell Death to Prevent Inflammation. *Cell Rep.* **27**, 2679–2689 (2019). e2673.
32. Miura, K., Karasawa, H. & Sasaki, I. cIAP2 as a therapeutic target in colorectal cancer and other malignancies. *Expert Opin. Ther. Targets* **13**, 1333–1345 (2009).
33. Nagata, M. et al. Overexpression of cIAP2 contributes to 5-FU resistance and a poor prognosis in oral squamous cell carcinoma. *Br. J. Cancer* **105**, 1322–1330 (2011).
34. Scomazzon, S. P. et al. The Zinc-Finger AN1-Type Domain 2a Gene Acts as a Regulator of Cell Survival in Human Melanoma: Role of E3-Ligase cIAP2. *Mol. Cancer Res.* **17**, 2444–2456 (2019).
35. Duvefelt, C. F. et al. Increased resistance to proteasome inhibitors in multiple myeloma mediated by cIAP2–implications for a combinatorial treatment. *Oncotarget* **6**, 20621–20635 (2015).
36. Wu, H. H. et al. cIAP2 upregulated by E6 oncoprotein via epidermal growth factor receptor/phosphatidylinositol 3-kinase/AKT pathway confers resistance to cisplatin in human papillomavirus 16/18-infected lung cancer. *Clin. Cancer Res.* **16**, 5200–5210 (2010).
37. Hu, X. et al. Cul4 E3 ubiquitin ligase regulates ovarian cancer drug resistance by targeting the antiapoptotic protein BIRC3. *Cell Death Dis.* **10**, 104 (2019).
38. Frazzi, R. BIRC3 and BIRC5: multi-faceted inhibitors in cancer. *Cell Biosci.* **11**, 8 (2021).
39. Niwa, N. et al. TNFAIP2 expression induces epithelial-to-mesenchymal transition and confers platinum resistance in urothelial cancer cells. *Lab. Investig.* **99**, 1702–1713 (2019).
40. Asaka, R. et al. Sirtuin 1 promotes the growth and cisplatin resistance of endometrial carcinoma cells: a novel therapeutic target. *Lab. Investig.* **95**, 1363–1373 (2015).
41. Dasari, S. & Tchounwou, P. B. Cisplatin in cancer therapy: molecular mechanisms of action. *Eur. J. Pharmacol.* **740**, 364–378 (2014).
42. Cai, Y., Yan, X., Zhang, G., Zhao, W. & Jiao, S. The predictive value of ERCC1 and p53 for the effect of panobinostat and cisplatin combination treatment in NSCLC. *Oncotarget* **6**, 18997–19005 (2015).
43. Lin, C. Y. et al. Demethoxycurcumin sensitizes the response of non-small cell lung cancer to cisplatin through downregulation of TP and ERCC1-related pathways. *Phytomedicine* **53**, 36 (2019). 28.

44. Rosell, R., Lord, R. V., Taron, M. & Reguart, N. DNA repair and cisplatin resistance in non-small-cell lung cancer. *Lung Cancer* **38**, 217–227 (2002).
45. Deben, C. et al. Hypoxia-Induced Cisplatin Resistance in Non-Small Cell Lung Cancer Cells Is Mediated by HIF-1α and Mutant p53 and Can Be Overcome by Induction of Oxidative Stress. *Cancers* **10**, 126 (2018).
46. Fischer, C. et al. Panobinostat reduces hypoxia-induced cisplatin resistance of non small cell lung carcinoma cells via HIF-1α destabilization. *Mol. Cancer* **14**, 4 (2015).
47. Gao, Z. J., Yuan, W. D., Yuan, J. Q., Yuan, K. & Wang, Y. Downregulation of HIF 2α Reverse the Chemotherapy Resistance of Lung Adenocarcinoma A549 Cells to Cisplatin. *Med. Sci. Monit.* **24**, 1104–1111 (2018).
48. Pandey, N. et al. Allicin Overcomes Hypoxia Mediated Cisplatin Resistance in Lung Cancer Cells through ROS Mediated Cell Death Pathway and by Suppressing Hypoxia Inducible Factors. *Cell Physiol. Biochem.* **54**, 748–766 (2020).
49. Huang, S. et al. Metformin reverses chemoresistance in non-small cell lung cancer via accelerating ubiquitination-mediated degradation of Nrf2. *Transl. Lung Cancer Res.* **9**, 2337–2355 (2020).
50. Wang, H. et al. Interplay of MKP-1 and Nrf2 drives tumor growth and drug resistance in non-small cell lung cancer. *Aging* **11**, 11329–11346 (2019).
51. Lan, D. et al. Exogenous glutathione contributes to cisplatin resistance in lung cancer A549 cells. *Am. J. Transl. Res.* **10**, 1295–1309 (2018).

FUNDING

This research was funded by the National Natural Science Foundation of China (No. 81802759, 81871231), the China Postdoctoral Science Foundation Funded Project (No. 2019M652312), and the Qingdao Postdoctoral Application Research Project.

AUTHOR CONTRIBUTIONS

C.L. and B.L. designed the study. C.L., Z.C., and X.D. performed the experiments and analyzed the data. C.L. wrote the paper. Y.Q. edited the paper. All authors read and approved the final paper.

COMPETING INTERESTS

The authors declare no competing interests.

ETHICS APPROVAL

Informed consent was obtained from all patients before inclusion in the study.

ADDITIONAL INFORMATION

Correspondence and requests for materials should be addressed to Yun Qiao or Bing Li.